

Sharp Rigid to Floppy Phase Transition Induced by Dangling Ends in a Network Glass

Y. Wang, J. Wells,* D. G. Georgiev, and P. Boolchand

Department of ECECS, University of Cincinnati, Cincinnati, Ohio 45221-0030

Koblar Jackson

Department of Physics, Central Michigan University, Mt. Pleasant, Michigan 48858

M. Micoulaut

Laboratoire de Physique Theorique des Liquides, Universite Pierre et Marie Curie, Boite 121, 4 Place Jussieu, 75252 Paris, Cedex 05, France

(Received 29 March 2001; published 16 October 2001)

The count of Lagrangian bonding constraints $n_c(y)$ in ternary $\text{Ge}_{25}\text{S}_{75-y}\text{I}_y$ glasses ($0 < y < 0.30$) is established from the molecular structure using Raman scattering and first-principles cluster calculations. The results show that $n_c(y)$ decreases to 3 as y increases close to $y_c = 0.162(3)$, where a *sharply* defined *global minimum* in the nonreversing heat flow, $\Delta H_{\text{nr}}(y)$ near T_g , is observed in scanning calorimetry. Here we have a *rigidity transition* induced by *I dangling ends*, with its sharpness resulting from the absence of *self-organization* in the random network.

DOI: 10.1103/PhysRevLett.87.185503

PACS numbers: 61.43.Fs, 63.50.+x

In 1788, Lagrange introduced [1] the notion of constraints and generalized coordinates in mechanics. Almost a century later, Maxwell used mechanical constraints to examine [2] the stability of macroscopic structures such as trusses and bridges. In the early 1980s, Phillips recognized [3] that in covalent solids, *valence forces* [bond stretching (bs) and bond bending (bb)] between atoms can also serve as independent *mechanical constraints*. A normal mode analysis of such solids by Thorpe showed [4] that the count of zero-frequency solutions (floppy modes) of the dynamical matrix actually vanishes when the number of Lagrangian bonding constraints per atom, n_c , increases to 3, the degrees of freedom per atom in 3D. These simple but powerful ideas have led to the prediction of a *rigidity transition* in random networks that has served as a paradigm [5] of percolative transitions in disordered condensed matter. The phase transition has been confirmed [6] in numerical simulations on generic random networks and the underlying elastic constant power laws have been established with increasing precision to discover that the mean-field results for the transition are remarkably accurate. On the other hand, experiments on binary and ternary chalcogenide glasses have recently shown the existence [7–9] of *two* (transitions) instead of *one* transition, thus suggesting that the elegant construction of mean-field constraint counting alone may be insufficient to describe the richness of the underlying phase transitions observed in glasses. Indeed, Raman scattering and T -modulated scanning calorimetry (MDSC) results on Si (or Ge)-Se, As-Ge-Se glasses suggest evidence [10] for the growth of a *self-organized intermediate phase* between the *floppy* and *stressed rigid* phases, for which independent evidence [11] is suggested from numerical simulations.

It was therefore of special interest to encounter a glass system where the rigid to floppy transition appears to be

almost completely described by mean-field theory. In this Letter, we report on the molecular structure of ternary $\text{Ge}_{0.25}\text{S}_{0.75-y}\text{I}_y$ glasses from Raman scattering experiments and first-principles cluster calculations. The results show $n_c(y) = 3$ when y is close to 0.162(3), a composition where a global minimum in the nonreversing heat flow, $\Delta H_{\text{nr}}(y)$ is observed in MDSC measurements. The observation constitutes direct evidence of a *rigid to floppy transition* induced by the *onefold coordinated* I atoms [12]. A novel aspect of the transition here is that it is unusually *sharp* and occurs close to the predicted mean-field value [13], features not observed previously [7–11].

The glasses were synthesized by reacting 99.99% pure elemental Ge, S, and GeI_4 as the starting materials, slowly (1 °C/min) heating up to 950 °C and equilibrating the melts close to the liquidus prior to a water quench. The glass transition temperature, $T_g(y)$, was measured at 1 °C/100 s modulation rate and 3 °C/min scan rate using a model 2920 MDSC instrument from TA Instruments, Inc., and show, in general, a monotonic decrease with y [Fig. 1 (inset)] with a narrow region near $y = 0.17$ where a sharp drop in T_g occurs. In a MDSC scan, one routinely deconvolutes [7–10] the total heat flow endotherm near T_g into a reversing part, \dot{H}_r , and a nonreversing part, \dot{H}_{nr} . Figure 1 reproduces the $\Delta H_{\text{nr}}(y)$ trend, which shows a sharply defined and deep minimum at $y = y_c = 0.162(3)$, or $\bar{r} = \bar{r}_c = 2.34$. Here the mean coordination number $\bar{r} = 2.5 - y$ and is obtained by taking the coordination numbers of Ge, S, and I to be 4, 2, and 1, respectively.

Raman scattering results (unpolarized) taken in a backscattering geometry using 647.1 nm radiation loosely focused to a 1 mm spot size appear in Fig. 2. Details of the setup appear elsewhere [7,8]. At $y = 0$, one observes [7] modes of corner-sharing (CS) and edge-sharing (ES) $\text{Ge}(\text{S}_{1/2})_4$ tetrahedra ($m = 0$) at $\nu_{\text{CS}}(0) = 341 \text{ cm}^{-1}$

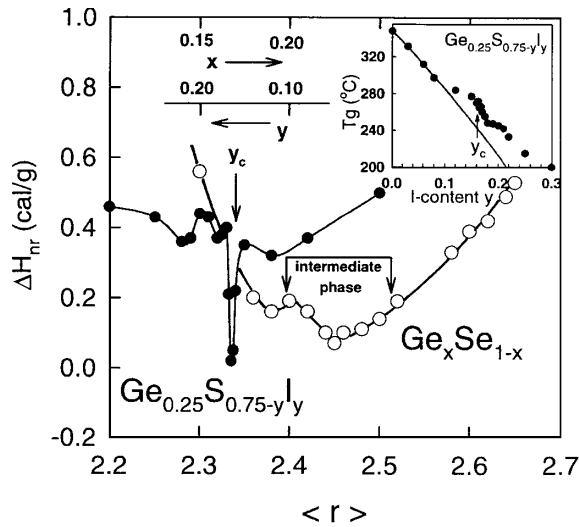


FIG. 1. Inset shows the $T_g(y)$ variation in titled glasses and the solid line is the prediction of SAT. The figure gives a variation of the nonreversing heat flow term, ΔH_{nr} , as a function of \bar{r} in the present ternary (\bullet) and the Ge-Se binary (\circ) (Ref. [7]). The arrows delineate the region of self-organization (Ref. [10]).

and at $\nu_{ES} = 370 \text{ cm}^{-1}$, respectively. The line shapes reveal new modes [14] (Fig. 2) of mixed $\text{Ge}(\text{S}_{1/2})_{4-m}\text{I}_m$ tetrahedra, $m = 1, 2, 3$, and 4, with increasing I content at about 240, 230, 185, and 155 cm^{-1} , respectively. These modes are found to be strongly polarized while the one at 260 cm^{-1} is depolarized. By deconvoluting the observed line shapes to an appropriate superposition of Gaussians, we have also obtained the mode frequency variation of the CS mode of the $m = 0$ species $\nu_{CS}(y)$ [Fig. 3(b)],

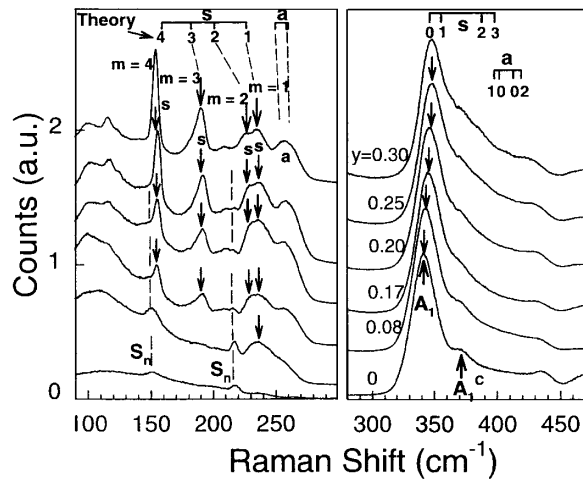


FIG. 2. Raman line shapes observed in the present ternary showing modes of CS $\text{Ge}(\text{S}_{1/2})_{4-m}\text{I}_m$ tetrahedra ($m = 1, 2, 3$, and 4) evolving with increasing iodine concentration in the low-frequency regime (left panel) and blueshift of the CS mode of $m = 0$ tetrahedra in the high-frequency regime (right panel). The label $s \equiv$ symmetric mode (polarized); $a \equiv$ antisymmetric (depolarized). The theoretically predicted mode frequencies from first-principles calculations are shown as vertical bars on top. S_n designates modes of S chains.

and the matrix element corrected (discussed later) normalized concentrations of the mixed tetrahedra $N_m(y)/N$ [Fig. 3(a)]. The concentrations of the mixed ($m = 1, 2$, and 3) tetrahedra increase at the expense of those of the pure tetrahedra ($m = 0$) with increasing I content. A comparison of the observed trends with those inferred from combinatorial calculations [15] [the solid lines in Fig. 3(a)] suggests that I replacement of bridging S atoms of the backbone proceeds almost *stochastically* up to $y = 0.20$. At higher $y (>0.20)$, this behavior is, however, interrupted as $m = 3$ and 4 units grow preferentially.

The $T_g(y)$ variation has been analyzed by stochastic agglomeration theory (SAT) [16]. The theory relates an increase in melt viscosity (or relaxation time) to agglomeration of specific local structural configurations ($m = 0, 1, 2, 3$, and 4 units in our case), and T_g is identified with the T where the agglomeration process freezes [17]. The solid line in the Fig. 1 inset gives the $T_g(y)$ prediction for the case when $m = 0, 1, 2$ units are considered in the agglomeration, and, as expected, nicely reproduces the observed trend since these are the only units populated at low y . At higher $y (>0.15)$,

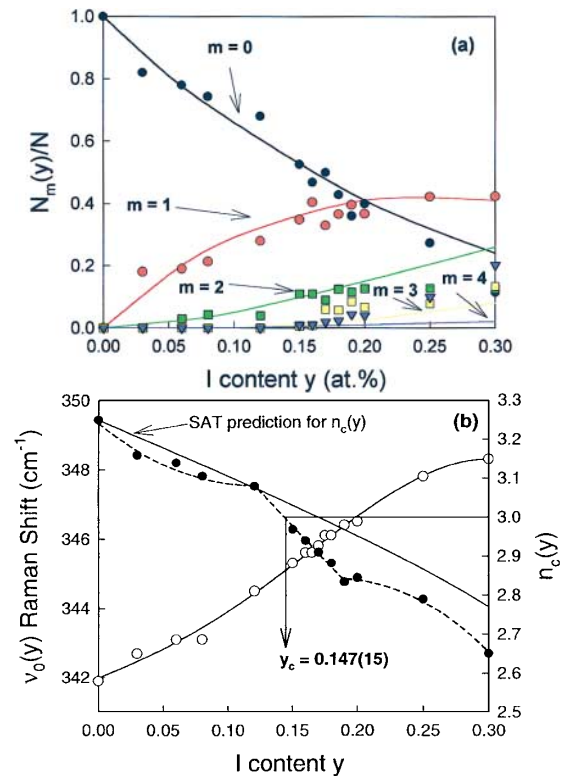


FIG. 3. (a) (color) Concentrations $N_m(y)/N$ of the mixed tetrahedra, $m = 0$ (dark circles), $m = 1$ (red circles), $m = 2$ (green squares), $m = 3$ (yellow squares), and $m = 4$ (blue triangles) plotted as a function of y . The solid curves are the predictions of the combinatorial calculation (Ref. [15]) and are not a fit to the data points. (b) Raman mode frequency (open circles) variation $\nu_0(y)$ of $m = 0$ units and the Raman count of $n_c(y)$, (solid circles) calculated from Eq. (2), plotted as a function of I content. The solid line is the prediction of $n_c(y)$ from SAT.

$m = 3$ units must also be considered, thus substantially increasing the range of possibilities for agglomeration, a point of ongoing investigations.

First-principles calculations [18,19] based on density functional theory (DFT) were carried out to predict the Raman mode frequencies and strengths for $\text{Ge}(\text{S}_{1/2})_{4-m}\text{I}_m$ tetrahedra, with $m = 0, 1, 2, 3$ and 4. The calculations made use of local orbital basis sets and a mixed pseudopotential/all-electron formalism [19]. H atoms were used to terminate dangling bonds so that all the S atoms in the models are twofold coordinated. Each cluster model was first relaxed to its minimum energy geometry and the full vibrational spectrum was calculated using a standard, finite-difference approach for building the force constant matrix [18,20]. The Raman intensity of each vibrational mode was computed using a new DFT-based approach [18] that was recently used to successfully model the Raman spectrum of GeSe_2 and GeS_2 [21]. The calculated Raman-active bond-stretching modes of the $\text{Ge}(\text{S}_{1/2})_{4-m}\text{I}_m$ tetrahedra appear in Table I. The modes are labeled (Table I, Fig. 2) symmetric (s) and asymmetric (a) according to whether the stretches of the various bonds are in phase or out of phase, respectively. The total number of modes (symmetric + asymmetric) in each case is four, corresponding to the four bonds of a tetrahedron. As m increases from 0 to 3, the frequency of the upper mode increases from 347 to 400 cm^{-1} while the frequency of the lower mode decreases from 226 to 183 cm^{-1} . The latter modes are clearly resolved in the observed line shapes (Fig. 2) and permit the integrated mode intensities to be established. The m -unit concentrations, $N_m(y)/N$, of the network building blocks [Fig. 3(a)] were then deduced by

TABLE I. Predicted Raman mode frequencies and scattering strengths of the mixed $\text{Ge}(\text{S}_{1/2})_{4-m}\text{I}_m$ units using first-principles calculations (Refs. [16–18]).

Unit m	Symmetric Mode		Asymmetric Mode	
	ω (cm^{-1})	I^{Ram} (Δ^4/amu)	ω (cm^{-1})	I^{Ram} (Δ^4/amu)
0	347	49.5	402	6.2
			412	8.6
			412	8.6
1	226	13.5	398	8.4
			358	38.7
2	202	23.6	251	3.1
			387	20.7
3	183	26.4	260	3.7
			400	14.7
4	159	27.6	261	4.1
			261	4.1
			261	4.1

normalizing the integrated intensities by the mode cross sections (Table I).

Our interpretation of the results is as follows. As in the chalcogenides [7–10], the global minimum in $\Delta H_{\text{nr}}(y)$ (Fig. 1) provides evidence of the rigid to floppy transition at $y_c = 0.162(3)$ or $\bar{r}_c = 2.338(3)$. ΔH_{nr} measures the latent heat (configurational energy change) between the glassy and liquid states, and it vanishes when the network is optimally constrained, i.e., $n_c = 3$. The location ($\bar{r} = 2.34$) and *narrow width* ($\Delta\bar{r} < 0.01$) of the rigidity transition are both consistent with a *stochastic evolution* of the network with increasing I content, as independently inferred above from the $T_g(y)$ trends (Fig. 1, inset) analyzed by SAT [16]. The mean-field prediction [13] of the rigidity transition in a random network having a finite fraction n_1/N of *onefold coordinated atoms* introduces a shift of the phase transition from the magic number [3,4] of 2.40 to a lower value that is given by

$$\bar{r}_c = 2.40 - 0.4(n_1/N). \quad (1a)$$

For the present $\text{Ge}_{25}\text{S}_{75-y}\text{I}_y$ ternary, the phase transition is then predicted to occur at a critical concentration y_c , given by

$$2.5 - y_c = 2.40 - 0.4y_c \quad \text{or} \quad y_c = 1/6. \quad (1b)$$

The mean-field prediction [13] at $y_c = 0.166$ above is thus in excellent accord with the MDSC result of $y_c = 0.162(3)$.

The Raman results [Fig. 3(b)] provide crucial insights into features of the glass structure responsible for the sharp phase transition observed. The near stochastic evolution of network structure at $y < 0.20$ suggested by the results of Fig. 3a is the consequence of a *delicate balance* between competing effects; a Pauling *charge transfer effect* [22] that promotes I bonding with Ge to favor network formation, and a *local clamping (size) effect* [23] that leads to molecular phase separation. The Pauling *charge transfer effect* requires I ($\chi_p = \text{electronegativity} = 2.5$) to chemically bond with Ge ($\chi_p = 1.8$) rather than S ($\chi_p = 2.5$), *ensuring* that the I for S replacement proceeds *exclusively* in the rigid backbone. On the other hand, such a replacement also clamps *the backbone* [23] locally in addition to reducing the *global connectivity* (reflected in the T_g reduction) as dangling Ge-I ends form. The *local clamping* is the consequence of a 30% larger *covalent* radius of the iodine additive ($r_I = 1.33 \text{ \AA}$) in relation to the S substituent ($r_S = 1.02 \text{ \AA}$) and the *repulsive nonbonding* van der Waals (vdW) interactions that drive the *lone-pair bearing* I and S atoms *apart* ($r_{\text{vdW}} = 3.78 \text{ \AA}$, Ref. [24]). One thus finds a *blueshift* [Fig. 3(b)] of the CS mode frequencies [$\nu_0(y)$] of the $m = 0$ units but a *redshift* of modes of $m = 1-4$ units (Fig. 2) as the network softens. The sigmoidal dependence of $\nu_0(y)$ [Fig. 3(b)] reflects the *local clamping effect* of the backbone. At low y , $\nu_0(y)$ increases slowly at first ($y < 0.05$) and then rapidly ($y > 0.10$)

as the clamping effect manifests upon halogenation. At $y > 0.20$, $\nu_0(y)$ saturates because the rapid growth in the $m = 4$ units [Fig. 3(b)] provides stress relief as molecular phase separation ensues.

A rewarding feature of the Raman results is that they fix concentrations, N_m/N , of the various m units [Fig. 3(a)] which permits an estimate of the global Lagrangian bonding constraints. Using

$$n_c(y) = \frac{3}{4} \sum_m \frac{N_m(y)}{N} C_m + \frac{1}{2}, \quad (2)$$

where the sum extends over network-forming units ($m = 0, 1, 2,$ and 3) and $C_m = (22 - m)/(6 + m)$ represents [25] the count of *bs* and *bb* constraints per atom in a given m unit. In Eq. (2), the base glass ($\text{Ge}_{25}\text{S}_{75}$) is regarded to be made up of a rigid GeS_2 phase (first term) and a floppy S_n -chain phase (second term) with I for S replacement depleting the count of constraints in the GeS_2 phase. Figure 3(b) provides a plot of $n_c(y)$, and one finds that the phase transition, $n_c = 3$, occurs when $y_c = 0.147(15)$, close to the more accurate value $y_c = 0.162(3)$ observed in MDSC. The less accurate Raman value of y_c is not surprising given the uncertainties in measurements of the mode scattering strengths and the estimate of mode cross sections. Finally, a fourth independent means to establish y_c derives from the $T_g(y)$ trends analyzed by SAT. By using Eq. (2) and the SAT derived $N_m(y)/N$ values, we have also deduced the $n_c(y)$ variation and obtain $y_c = 0.169$ at $n_c = 3$ [Fig. 3(b)]. These results provide a direct test of the original principle [3,4], $n_c = 3$, used as the basis of the rigidity transition in random systems.

In summary, we have observed a *sharply defined rigidity transition* in a glass network induced by dangling ends. We have estimated the critical composition by two independent methods, both yielding good agreement with experiments. The best agreement is obtained by assuming that at the critical composition the I dopants are bonded to Ge but are otherwise randomly distributed and unaffected by clamping (size) effects. Such random distributions are rare and their presence explains the observed extreme narrowness of the thermally reversing window. This in turn implies that observation of wide thermally reversing windows in network glasses [7–10] is best understood in terms of network self-organization.

This work is supported by NSF Grants No. DMR-01-01808 (University of Cincinnati) and No. DMR-RUI-9972333 and No. DMR-MRI-9977582 (Central Michigan University). LPTL is Unité Mixte de Recherche CNRS No. 7600.

*Permanent address: Thomas Moore College, Crestview Hills, Kentucky 41017.

- [1] J. L. Lagrange, *Mechanique Analytique* (Paris, 1788).
- [2] J. C. Maxwell, *Philos. Mag.* **27**, 294 (1864).
- [3] J. C. Phillips, *J. Non-Cryst. Solids* **34**, 153 (1979).
- [4] M. F. Thorpe, *J. Non-Cryst. Solids* **57**, 355 (1983).
- [5] J. C. Phillips, in *Phase Transitions and Self-Organization in Electronic and Molecular Glasses*, edited by J. C. Phillips and M. F. Thorpe (Kluwer/Plenum, New York, 2001), p. 1.
- [6] M. F. Thorpe *et al.*, in *Insulating and Semiconducting Glasses*, edited by P. Boolchand (World Scientific, Singapore, 2000), p. 95.
- [7] X. W. Feng *et al.*, *Phys. Rev. Lett.* **78**, 4422 (1997).
- [8] D. Selvanathan *et al.*, *Phys. Rev. B* **61**, 15 061 (2000).
- [9] Y. Wang *et al.*, *Europhys. Lett.* **52**, 633 (2000).
- [10] P. Boolchand *et al.*, in *Phase Transitions and Self-Organization in Electronic and Molecular Glasses* (Ref. [5]), p. 65; see also P. Boolchand *et al.*, *J. Optoelectron. Adv. Mater.* **3**, 703 (2001).
- [11] M. F. Thorpe *et al.*, *J. Non-Cryst. Solids* **266–269**, 859 (2000).
- [12] S. A. Dembovsky *et al.*, *Neorg. Mater.* **7**, 328 (1971).
- [13] P. Boolchand and M. F. Thorpe, *Phys. Rev. B* **50**, 10 366 (1994).
- [14] L. Koudelka and M. Piaricick, *J. Non-Cryst. Solids* **97–98**, 1271 (1987); See also J. Heo and J. D. MacKenzie, *J. Non-Cryst. Solids* **111**, 29 (1989).
- [15] The probability P_m for the occurrence of a given m unit at random upon adding y fraction of I is given as, $P(m, y) = \frac{4!}{m!(4-m)!} y^m (1-y)^{4-m}$. The solid lines in Fig. 3(a) show a plot of $P(m, y)$ for various m .
- [16] M. Micoulaut, *Eur. Phys. J. B* **1**, 277 (1998); see also R. Kerner and M. Micoulaut, *J. Non-Cryst. Solids* **210**, 298 (1997).
- [17] M. Micoulaut, in *Phase Transitions and Self-Organization in Electronic and Molecular Glasses* (Ref. [5]), p. 143.
- [18] M. R. Pederson and K. A. Jackson, *Phys. Rev. B* **41**, 7453 (1990).
- [19] A. Briley *et al.*, *Phys. Rev. B* **58**, 1786 (1998).
- [20] D. V. Porezag and M. R. Pederson, *Phys. Rev. B* **54**, 7830 (1996).
- [21] K. Jackson *et al.*, *Phys. Rev. B* **60**, R14985 (1999).
- [22] L. Pauling, *Nature of the Chemical Bond* (Cornell University Press, Ithaca, NY, 1960), p. 85.
- [23] S. Alexander, *Phys. Rep.* **296**, 65 (1998); E. Courtens *et al.*, *Solid State Commun.* **117**, 187 (2000).
- [24] B. Douglas, D. McDaniel, and J. Alexander, *Concepts and Models of Inorganic Chemistry* (Wiley, New York, 1994), 3rd ed., p. 102.
- [25] For a $\text{Ge}(\text{S}_{1/2})_{4-m}\text{I}_m$ unit, $n_c = [7 + (4 - m) + m/2]/(3 + m/2)$ or $(22 - m)/(6 + m)$, obtained by counting the number of *bs* and *bb* constraints per atom, and yields 3.67, 3.00, 2.50, 2.11, and 1.80 at $m = 0, 1, 2, 3,$ and 4 , respectively.